Generalized HARDI Invariants by Method of Tensor Contraction

Yaniv Gur and Chris R. Johnson
SCI Institute, University of Utah

Introduction

We propose a 3D object recognition technique to construct rotation invariant feature vectors for high angular resolution diffusion imaging (HARDI).

- This method uses the expansion of spherical functions by means of spherical harmonics (SH).
- It is based on generating rank-1 contravariant tensors using the SH coefficients and contracting them with covariant tensors to obtain rotation invariants.
- The proposed technique enables the systematic construction of rotation invariants for spherical functions (e.g. orientation distribution functions - ODFs) of any expansion order using simple mathematical operations.
- These invariants are more robust to noise than other invariants perviously used in medical image analysis.

Spherical Harmonics Expansion

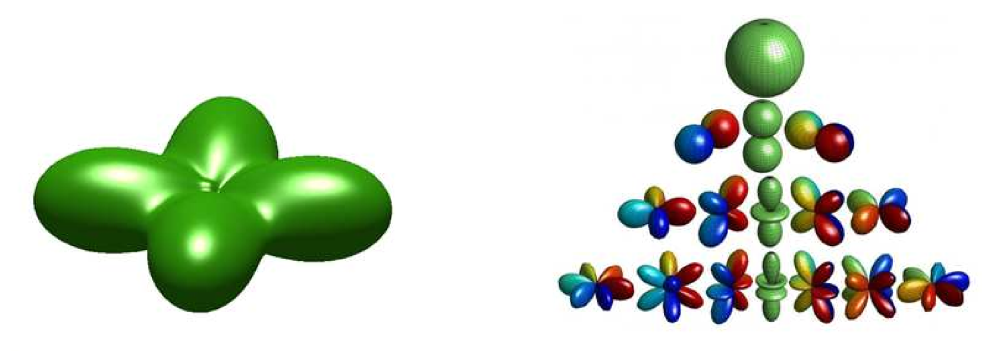

$$f(\theta,\varphi)=\sum_{l=0}^{L}\sum_{m=-l}^{l} c_l^m Y_l^m$$

- While there are no restrictions on the expansion order, L, most HARDI reconstruction techniques are based on even order expansions using real c_l^m's.
- The method presented here is based on complex SH representation. Therefore, we map the real coefficients to the complex domain as follows:

$$c_l^m=\begin{cases}\frac{1}{\sqrt{2}}(\hat{c}_{lm}+i\hat{c}_{l\,-m}) & \text{if } m>0\\ \hat{c}_{l0} & \text{if } m=0\\ (-1)^m(\hat{c}_l^{-m})^* & \text{if } m<0,\end{cases}$$

where $\hat{c}_{lm}$ denotes the real coefficients, and $*$ stands for the complex conjugate.

Power Spectrum SH Descriptors

I-invariants

A contraction of the SH coefficients with their complex conjugates

$$I_l=c_l^m c_{lm}=\sum_{m=-l}^{l} c_l^m (c_l^m)^*.$$

The power spectrum SH descriptors are used in various shape and image analysis tasks [1, 2], as well as in clinical studies [3].

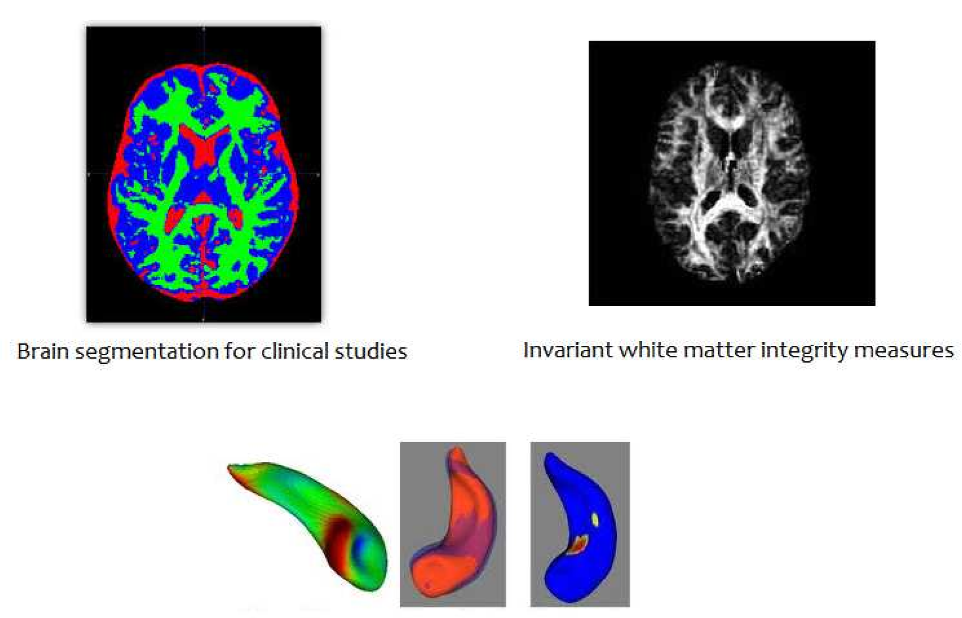

Rotation Invariants using CG coefficients

- The subspace $V_l=\mathrm{Span}\{Y_l^{-l},Y_l^{-l+1},\ldots,Y_l^{l-1},Y_l^l\}$ is globally rotational invariant.
- As proposed in [4], using the Clebsch-Gordan (CG) coefficients contravariant rank-1 tensors in V_l can be generated as follows:

$$\begin{aligned}T^m_{l,l_1,l_2}&=k^{m,m_1,m_2}_{l,l_1,l_2}c_{l_1m_1}c_{l_2m_2}\\&=\sum_{m_1=-l_1}^{l_1}\sum_{m_2=-l_2}^{l_2}k^{m,m_1,m_2}_{l,l_1,l_2}(c_{l_1}^{m_1})^*(c_{l_2}^{m_2})^*,\end{aligned}$$

where $k^{m,m_1,m_2}_{l,l_1,l_2}$ are the CG coefficients.

- These tensors can be contracted with the SH coefficients to create rotation invariants:

J-invariants

A contraction of the T-tensors with the complex conjugates of the SH coefficients

$$J_{l,l_1,l_2}=T^m_{l,l_1,l_2}c_{lm}=\sum_{m=-l}^{l}T^m_{l,l_1,l_2}(c_l^m)^*.$$

- In addition, they can be contracted with each other to construct a different set of invariants:

K-invariants

A contraction of the T-tensors with their complex conjugates

$$K_{l,l_1,l_2,l_3,l_4}=T^m_{l,l_1,l_2}T_{l,l_3,l_4,m}=\sum_{m=-l}^{l}T^m_{l,l_1,l_2}(T^m_{l,l_3,l_4})^*.$$

- The process of generating tensors and contracting them can be continued repeatedly to generate as many invariants as needed.
- The conditions under which these invariants can be computed are $|l_1-l_2|\le l\le(l_1+l_2)$ for J, and the additional condition $|l_3-l_4|\le l\le(l_3+l_4)$ for K, whereas the I invariants can be computed for any l.

Simulated Data Results

- Using constrained spherical deconvolution (CSD) [5] we generated three groups of 100 noisy FODs (SNR=20, L=8). The FODs were randomly rotated in space.
- Each group of FODs represents one, two, or three crossing fibers.
- For each FOD we computed 10 different invariants (5 for each invariant type): I_l, $l=0,2,\ldots,8$ and $J_{0,2,2}$, $J_{2,2,2}$, $J_{4,2,2}$, $J_{6,4,4}$, $J_{8,4,4}$.
- We showed that the J-invariants are more robust to noise than the I-invariants by mapping the FODs to a 3D feature space using the first three invariants of I and J.
- We used PCA to compare the performance of these invariants using the complete set of invariants we generated.

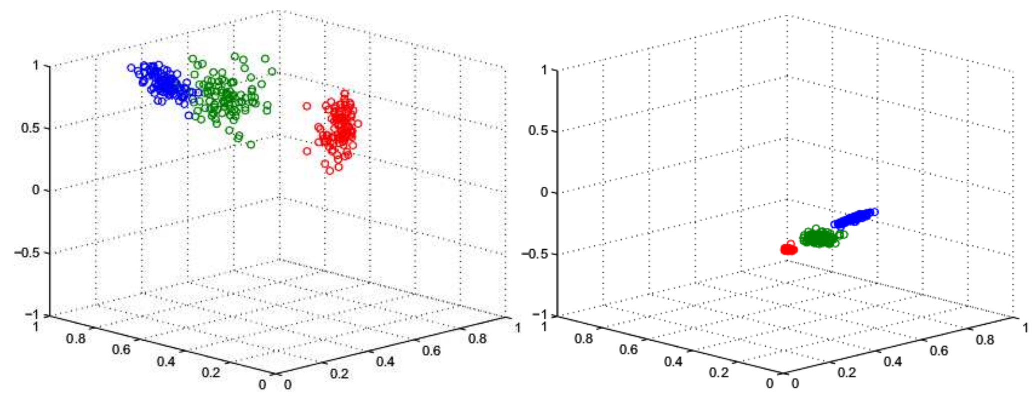

Figure 1: Number of fibers classification using the I-invariants (left), and the J-invariants (right). The point clouds correspond to one fiber (blue), two fibers (green), and three fibers (red).

		Variance				
1F	I	0.0336	0.0176	0.0065	0.0040	0.0013
	J	0.0190	0.0063	0.0011	0.0008	0.0008
2F	I	0.0246	0.0193	0.0153	0.0049	0.0040
	J	0.0063	0.0038	0.0034	0.0019	0.0007
3F	I	0.0263	0.0125	0.0074	0.0052	0.0035
	J	0.0040	0.0030	0.0011	0.0010	0.0007

Table 1: Variance comparisons using PCA. The labels 1F, 2F and 3F correspond to one, two, or three fibers, respectively. The labels I and J indicate the invariant type, and each row presents the vector of invariants beginning with $l=0$ (left).

ISBI Phantom Results

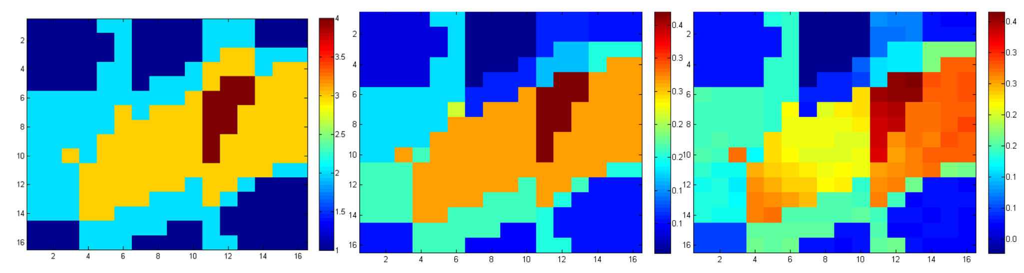

Figure 2: Voxel-wise classification of the simulated ISBI'12 challenge phantom. From left to right: the ground-truth number of fibers map, the same map segmented according to the principal diffusivities, and voxel-wise classification using the J-invariants.

Brain Data

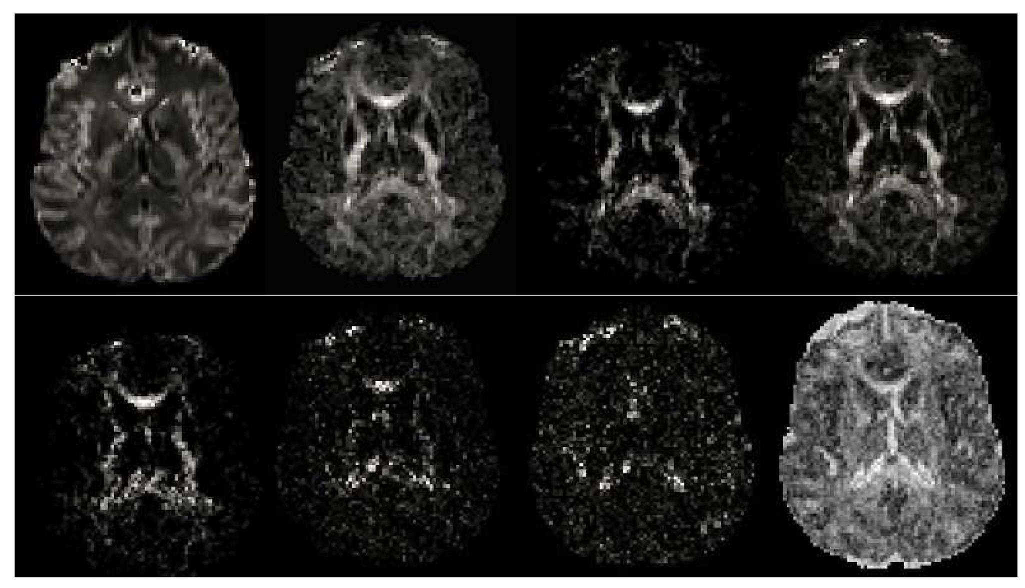

Figure 3: Maps of the J-invariants extracted from in vivo brain data. Top (L to R): $J_{0,0,0}$, $J_{0,2,2}$, $J_{2,2,2}$, and $J_{2,2,0}$. Bottom: $J_{4,2,2}$, $J_{4,4,2}$, $J_{6,4,4}$, and GFA.

References

[1] G. Gerig, M. Styner, D. Jones, D. Weinberger and J. Lieberman, "Shape analysis of brain ventricles using SPHARM", Mathematical Methods in Biomedical Image Analysis (MMBIA 2001), Pages 171-178, 2011.

[2] H. Skibbe and M. Reisert, "Rotation covariant image processing for biomedical applications", Computational and Mathematical Methods in Medicine, pp. 908-915, 2013.

[3] L. Bloy and R. Verma, "HARDI Based Pattern Classifiers for the Identification of White Matter Pathologies", in MICCAI'11, pp. 234-241, 2011.

[4] Gilles Burel and Hugues Hnocq, "Three-dimensional invariants and their application to object recognition", Signal Processing, vol. 45, no. 1, pp. 1-22, 1995.

[5] J-Donald Tournier, Fernando Calamante and Alan Connelly, "Robust determination of the fibre orientation distribution in diffusion MRI: Non-negativity constrained super-resolved spherical deconvolution", NeuroImage, vol. 35, pp. 1459–1472, 2007.

Acknowledgements

This work was funded in part by the NIH/NCRR Center for Integrative Biomedical Computing, P41RR12553